Nonlinear ultrasonic inspection of the effect of contaminants on material properties of epoxy-adhesive

Do-Kyung Pyun
Iowa State University
Lucas W. Koester
Iowa State, University
Daniel J. Barnard
Iowa State, University
Leonard J. Bond (bondlj@iastate.edu)
Iowa State University

Research Article

Keywords: epoxies, adhesive joints, contaminants, second harmonic generation, nonlinearity parameter

Posted Date: March 31st, 2022

DOI: https://doi.org/10.21203/rs.3.rs-1502609/v1

Draft paper for J. NDE **3/29/2022**

Title: Nonlinear ultrasonic inspection of the effect of contaminants on material properties of epoxy-adhesive

Authors: Do-Kyung Pyun[1], Lucas W. Koester[2], Daniel J. Barnard[2], and Leonard J. Bond[1,2]

1) Department of Aerospace Engineering, Iowa State University, Ames, USA

2) Center for Nondestructive Evaluation, Iowa State, University, Ames, USA

Key words: epoxies, adhesive joints, contaminants, second harmonic generation, nonlinearity parameter

Abstract

Adhesive joints have been an effective alternative to conventional mechanical fasteners for joining materials in the aerospace and automotive industries. Although adhesive joints have various advantages, including uniform stress distribution, lower weight, improved corrosion tolerance, and design flexibility, there can be various defects in adhesive joints, which have limited wider application. This paper investigates the effect of a contaminant on the chemical and mechanical properties of the epoxy-adhesive and seeks to determine if a SHG method can reliably detect and characterize the degree of contamination in the epoxy-adhesive. A contract based ultrasonic through-transmission method was used to measure nonlinearity and then the nonlinearity parameter was calculated using the measured fundamental and second harmonic frequency components in the signals. It was found that there is higher sensitivity to contaminant concentration, up to 1.5%, of the nonlinearity parameter than that for the sound velocity. These data were also found to correlate with changes in the mechanical hardness, which was measured by the Rockwell hardness testing, with different four levels of contamination. Differential scanning calorimetry (DSC) and the thermogravimetric analysis (TGA) were also conducted to assess the effect of the contaminant on thermal properties of the epoxy-adhesive. The DSC and TGA techniques were used to evaluate the curing reaction and the thermal stability of the epoxy-adhesive respectively.

Key words: epoxies, adhesive joints, contaminants, second harmonic generation, nonlinearity parameter

Corresponding author: Leonard J. Bond bondlj@iastate.edu

1. Introduction

Adhesive joints are an effective and potentially attractive alternative to conventional mechanical fasteners used to join similar or dissimilar materials in the aerospace industry. Adhesive joints have various advantages over fasteners, including uniform stress distribution, lower structure weight, improved corrosion tolerance, and design flexibility. In addition, the reduction in numbers of fasteners enables some forms of smart structures, such as embedded sensor systems [1]. The potential for reduced weight in aircraft, through the use of adhesive joints, also gives potential for higher fuel efficiency with reduced [2]. However, defects in adhesive joints can reduce strength, and the inability to reliably quantify strength has prevented such joints from use in a wider range of applications that would enable use of fewer fasteners.

Adhesive joints can exhibit various defects, including at the interfaces between adhesive and substrates and in bulk adhesive, that are due to poor fabrication processes and presence of foreign material introduced in manufacturing, and in-service damage [3]. To enable increased use of adhesive joints, it is necessary to detect these defects, reliably quantify strength and ensure uniform joint quality.

In looking in detail at the local structure found in adhesive joints there can be micro-scale defects at the micrometer (μm) scale, and these are in the form of voids and cracks, which are also stress concentrators and these are early-stage defects, with potential for growth in these joints. The detection and evaluation of such micro-scale defects, before they develop into macro-scale defects, can enable corrective actions to be taken that potentially enable an increase in structural lifetime and, and in the process, give a reduction in inspection cost. For example, since macro-scale defects in a system in fatigue can develop with about 20% of structural life remaining before fracture. The reliable detection of such micro-scale defects can reduce the potential for catastrophic failure in structures [4].

Although there have been advances in ultrasonic evaluation techniques used to detect micro-scale defects in adhesive joints, these have in general focused on detecting interfacial defects and delamination induced in-service [5-8], which are also known as dry contact kissing bonds [9]. Various studies have investigated such defects, and it appears that this is in part because such damage is relatively simpler to simulate in experimental samples [10,11]. Kissing bonds remain as one form of critical joint defects defined as surfaces are in intimate mechanical contact between adhesive and substrates, but there is little or no bond strength [12].

Micro-scale defects can come in several forms, in addition to kissing bonds, through the introduction of various contaminations during the manufacturing process. Contaminants can, in general, cause two types of micro-scale defects in the adhesive joints as shown in Fig. 1. Firstly, these can be in the form of interfacial defects, also known as contaminant or liquid layer kissing bonds [9], where the contaminants remain at the interface between the substrates and adhesive [9,13,14]. Secondly, if contaminants are mixed into bulk epoxy-adhesive, they will generally change properties and cause poor cohesion, which is seen as a degradation of the strength of the adhesive materials itself [15,16]. Prior studies have focused on detection and characterization of the kissing bonds based on several contaminants, including silicone-based release agents [17], oils [18], sand [14], and polytetrafluoroethylene (PTFE) [19] and ethylene tetrafluoroethylene (ETFE) films [20]. In seeking to detect these contaminants and quantify

performance of such defective bonds various NDE techniques have been investigated. These techniques include infrared thermography [19], digital image correlation (DIC) [20], micro-wave imaging [21], vibro-acoustic modulation [22], and ultrasonic resonance spectroscopy [14]. In reviewing the various approaches, each gave images and showed some possibility for the detection and mapping of kissing bonds, but they all still have their own limitations in the measurements and alternate approaches remain of interest.

Nonlinear ultrasonic techniques are one family of methods that have been demonstrated to have some potential for effective detection and characterization of some micro-scale defects [23]. Such nonlinear ultrasonic techniques are based on wave modulation generated when incident ultrasonic waves interact with the micro-structurally changed materials, such as micro-scale defects, which induce various nonlinear interaction phenomena [24-29]. Second harmonic generation (SHG) is one of the typical nonlinear phenomena that occurs when a finite amplitude ultrasonic wave is propagating through materials, and there is energy transfer from the fundamental into the higher harmonic components, as a result of the wave distortion due to energy interacting with the micro-structural changes encountered in the materials [30-32].

In quantifying such interactions the nonlinearity parameter (β) is used, which is a ratio of the amplitude of the fundamental and second harmonic components, and this has been shown to be directly related to micro-structural changes in materials [33,34]. The SHG method has been used as a metric to evaluate various micro-scale defects and damage in materials. Cantrell and Yost [35] used the nonlinearity parameter to characterize fatigue damage in aluminum alloy 2024-T4 and they showed that an increase in the nonlinearity parameter is related to the growth of dislocation dipoles during fatigue cycles. Ruiz et al. [36] applied nonlinear Rayleigh wave to evaluate early thermal damage in 2205 duplex stainless steel. In this case the nonlinearity parameter is shown to be related to the precipitation of a sigma phase during thermal aging. In addition, Balasubramaniam et al. [37] used both second and third harmonic components to measure creep damage in copper. They employed low amplitude longitudinal ultrasonic waves and demonstrated that the nonlinear response is sensitive to creep-generated dislocations. For interfacial micro-scale defects, Barnard et al. [38] produces samples that simulated a partially closed interface in a copper-copper diffusion bond. It was shown that differences in interfacial strength can effectively be related to interface condition and evaluated using second harmonic generation.

The specific problem of kissing bonds at interfaces was considered by Brotherhood et al. [39] who investigated simulated dry contact kissing bonds in adhesively bonded joints. A linear ultrasonic and a high-power based nonlinear ultrasonic method, measuring the second harmonic component, were both used as a function of the contact pressure applied to the joint. The results showed that each method has their own sensitivity to certain states of the interface. The linear method is sensitive to defects when a higher contact pressure is applied. On the other hand, the nonlinear method is shown to be effective in detecting defects when a low contact pressure is applied to the kissing bonds. The use of a combination of linear and nonlinear methods appears to have potential to enhance the effectiveness of defect detection.

The various SHG measurements, which have demonstrated potential in various applications, have not yet been applied for the detection of poor cohesion induced by contaminants in the epoxy-adhesive, even though contaminant-based poor cohesion is one of the potential critical

defects identified in adhesive joints during manufacturing [16]. When contaminants are mixed into the epoxy-adhesive during the manufacturing processes, they will alter the chemical aspects of the epoxy structure, typically reducing the curing reaction, which deteriorates the mechanical properties of the epoxy, which will then cause a reduction in bond quality and strength and increase the risk of cohesive failure in adhesive joints.

This paper investigates the effect of a contaminant on the chemical and mechanical properties of the epoxy-adhesive and seeks to determine if a SHG method can reliably detect and characterize the degree of contamination in the epoxy-adhesive, expanding on preliminary data presented previously [40]. In manufacturing, release agents which are required to produce many adhesively jointed structures, are one possible source of critical contaminants in adhesively jointed structures. This material was used at low concentration in thick epoxy-adhesive samples. A contract based ultrasonic through-transmission method was used to measure nonlinearity and then the nonlinearity parameter was calculated using the measured fundamental and second harmonic frequency components in the signals.

In seeking to quantify the effectiveness of the SHG method, the variation in nonlinearity parameter was compared with corresponding changes in the sound velocity as a linear ultrasonic parameter used to detect the contaminant-based poor cohesion with varying contamination levels. It was found that there is higher sensitivity to contaminant concentration of the nonlinearity parameter than that for the sound velocity. These data were also found to correlate with changes in the mechanical hardness, which was measured by the Rockwell hardness testing, with different four levels of contamination. Differential scanning calorimetry (DSC) and the thermogravimetric analysis (TGA) were also conducted to assess the effect of the contaminant on thermal properties of the epoxy-adhesive. The DSC and TGA techniques were used to evaluate the curing reaction and the thermal stability of the epoxy-adhesive respectively [41,42]. A correlation between the nonlinearity parameter and the thermal, and mechanical properties of the epoxy-adhesive was found.

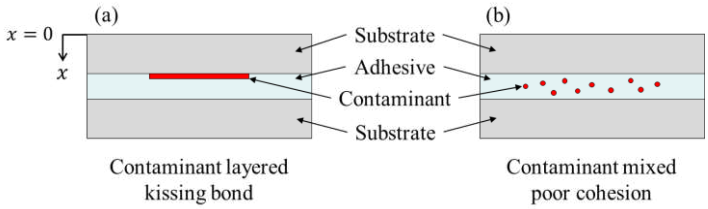

Fig. 1 Two types of contaminant-based micro-scale defects in general adhesive joints: (**a**) contaminant layered kissing bond and (**b**) contaminant mixed poor cohesion

2. Second harmonic generation

When a monochromatic ultrasonic wave with a finite amplitude is incident on micro-structurally changed materials, due to defects or damage, higher harmonic components are generated from the wave-material interaction that gives wave distortion [23]. It has been found that the second-order harmonic component has a larger amplitude than other higher harmonic

components and such interactions are dependent on the level change of material nonlinearity due to the micro-scale defects. As such this offers the potential that the SHG method is effective for certain classes of micro-scale defects [40].

The micro-scale defects that induce the nonlinear behavior in the ultrasound-material interactions can be described with the stress and strain relationship as given as equation 1. This relationship is limited to the second-order term as only the second harmonic component is employed in this analysis.

$$\sigma = E\varepsilon(1 + \beta\varepsilon) \tag{1}$$

where σ is the stress, E is the Young's modulus, ε is the strain, and β the nonlinearity parameter.

A one-dimensional monochromatic longitudinal wave propagating in the x-direction of materials (as defined in Fig. 1) can be described with equation 2. When this ultrasonic wave is incident on the nonlinear material, the resulting nonlinear wave equation can be obtained by combining equations 1 and 2 to give equation 3.

$$\rho \frac{\partial^2 u(x,t)}{\partial t^2} = \frac{\partial \sigma(x,t)}{\partial x} \tag{2}$$

$$\rho \frac{\partial^2 u(x,t)}{\partial t^2} = E \frac{\partial^2 u(x,t)}{\partial x^2} + 2E\beta \frac{\partial u(x,t)}{\partial x} \frac{\partial^2 u(x,t)}{\partial x^2} \tag{3}$$

where $u(x,t)$ is the displacement and ρ is the density.

To solve the nonlinear wave equation first-order perturbation theory is used and this gives the nonlinearity parameter (β) shown as equation 4 [43].

$$\beta = \frac{8}{k^2 x} \frac{A_2}{{A_1}^2} \tag{4}$$

where k is the wave number, A_1 is the displacement amplitude of the fundamental component, and A_2 is the displacement amplitude of the second harmonic component. The nonlinearity parameter is directly proportional to the amplitude of the second harmonic component, which is generated from the interaction with micro-scale defects in materials.

In an experiment if the measured samples have the same thickness and a fixed excitation frequency and pulse is used, the nonlinearity parameter can be simplified to the relationship given as equation 5 (a). In the experiments the amplitudes of the received electrical signals can be measured and used directly to give a relative nonlinearity parameter (β'), shown in equation 5 (b). In this case there is no requirement for additional calculation or corrections which are required a calibration process [44,45] to obtain the absolute displacement amplitude of each harmonic component in equation 5 (a).

The metric (β') can be used for the relative comparison of the level of the micro-structural change in materials at different contamination levels, as used in this study. Additionally, the use of the metric (β') can minimize the effects of the excitation amplitude and the coupling condition on the second harmonic measurements, when compared with those encountered in determining the absolute nonlinearity parameter (β) that is shown in equation 5 (a) [46].

$$\beta = \frac{A_2}{{A_1}^2} \tag{5 (a)}$$

$$\beta' = \frac{{A_2}'}{{A_1}'^2} \tag{5 (b)}$$

where ${A_1}'$ and ${A_2}'$ are the measured electrical signal amplitudes of the received fundamental and second harmonic components respectively.

3. Samples

A series of epoxy samples were fabricated in the form of short cylinders, approximately 25.4 mm in diameter and 8 mm thick. In curing of epoxy mixtures, it is the general process of the curing reaction, which determines the quality of the cured epoxy samples, and this is described below. The sets of samples were prepared for each ultrasonic measurements, and mechanical and thermal testing with varying levels of contamination.

3.1 Materials

The epoxy-adhesive used in this study was composed of the epoxy resin (EPO-FIX EMBEDDING RESIN, USA), and the hardener (EPO-FIX HARDENER, USA). The epoxy resin is based on bisphenol A diglycidyl ether (commonly abbreviated BADGE or DGEBA), which is the combination of bisphenol A and epichlorohydrin, and the hardener is based on triethylenetetramine (TETA) which is a primary aliphatic amine. The contaminant used was the release agent (BUEHLER RELEASE AGENT, USA) which is based on isooctane. Their chemical structures are shown in Fig. 2. The critical curing reaction for the synthesis of the epoxy resin and the hardener involves opening the epoxide ring of the resin by the active hydrogen in the amines of the hardener, which induces the polymerization in the mixture. Repeated reactions between the epoxy resin and hardener eventually form a three-dimensional epoxy structure which is the cross-linked network. Fig. 3 shows the general mechanism of the ring-opening polymerization for the epoxy network formation during the curing reaction between the epoxy resin and hardener [47].

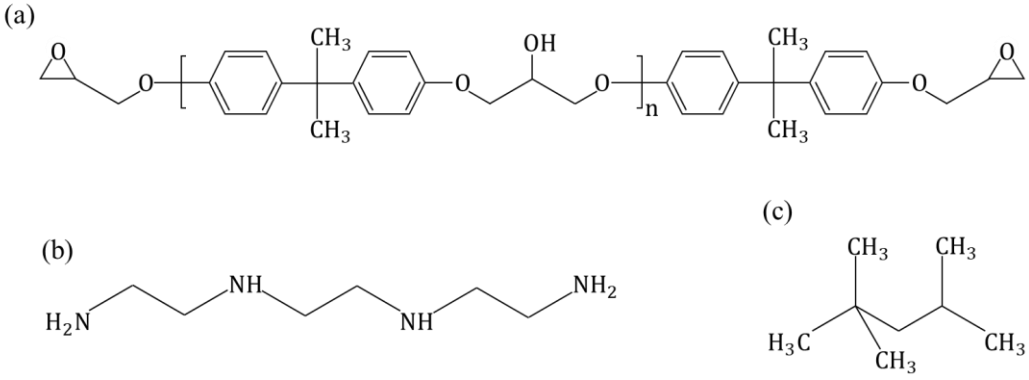

Fig. 2 Chemical structure of (**a**) the epoxy resin, (**b**) hardener, and (**c**) release agent

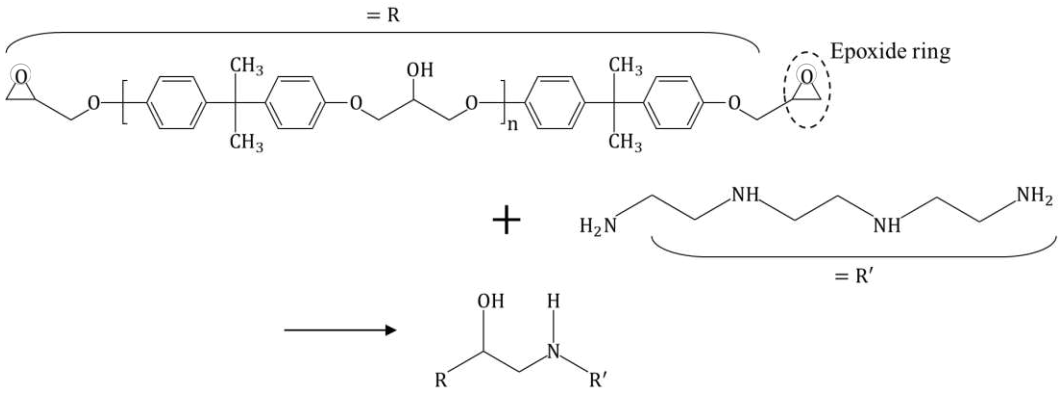

Fig. 3 General curing mechanism between the epoxy resin and primary hardener

3.2 Sample preparation

The epoxy resin and hardener were consistently mixed in the ratio of 28:3 parts by weight following the product preparation instructions. After this mixing, the release agent, used as the contaminant, was added into the mixture at the level of 0.5, 1.0, and 1.5% of the total weight of the mixture and the compounds were then completely mixed again for each of four samples, including the pure (uncontaminated) sample. The mixtures were degassed in a vacuum chamber to remove air bubbles entrained into the mixtures and poured into molds coated with a release agent in advance, and into alumina crucibles, to be used in subsequent testing after curing. The mixture in the molds is for ultrasonic measurements and hardness testing, and the mixture in the alumina crucibles is for thermal analyses. After pouring, the mixtures were again degassed and cured under vacuum at room temperature. For ultrasonic and hardness measurements, the thickness of the cured samples was set to 8 mm ($\pm$ 0.05 mm) with parallel surfaces and the surfaces of the samples were polished using a series of sandpapers (120, 320, 600, 1000, 2000, 3000, and 5000 grits) to smooth initial surface roughness.

4. Experiments

In experiments, using ultrasound, the sound velocity (c) and the relative nonlinearity parameter (β') obtained using the SHG method were measured, and data used to determine sensitivity to the levels of contamination. Also, to check the effects of contamination on change of the material properties of the epoxy samples, such as mechanical and thermal properties, mechanical hardness, and curing reaction and thermal stability were evaluated through the Rockwell hardness testing, and differential scanning calorimetry (DSC) and thermogravimetric analysis (TGA). The experimental details are set out below.

4.1 Second harmonics generation

A through-transmission ultrasonic experimental [40, 45] setup shown in Fig. 4 was used to measure the fundamental and second harmonic components for samples containing four different levels of contamination. A 17 cycles tone-burst signal, 800 mV peak-to-peak, was generated from the function generator (Agilent, USA) and then amplified through the high-power amplifier (RITEC GA-2500, USA). Before reaching the transmitting transducer, the signal passed through a 50 Ω terminator and the two stage low pass filters to give more consistent and reliable signals by removing the transient signal and the nonlinear effects due to the electronics in the experimental system. The stepped attenuator was also used to obtain several sets of data by varying the current output signals by changing the power. Based on this through-transmission method, a 5MHz commercial transducer (Olympus V110, USA) with 6.35 mm (0.25 inch) diameter, was used to transmit ultrasonic longitudinal waves, and a broad-band 10 MHz commercial transducer (Olympus V112, USA), with the same dimension was used as the receiver to increase sensitivity to the second harmonic frequency to detect both the fundamental and the second harmonic frequency components. The spectra for the transducers were measured. The center frequency of the transmitter is 5.68 MHz, with the -3 dB bandwidth being from 4.35 to 6.98 MHz, and the receiver has the center frequency of 6.81 MHz with the -3 dB bandwidth being from 4.29 to 9.91 MHz.

The fundamental frequency excited is set as 4.5 MHz, because this frequency can optimize the measurement by providing stable waveforms for the tone-burst signals and provide large amplitudes in the measured signals in the transmitter-receiver combination used in this study. The received time domain signals for the ultrasonic waves that propagated through the samples were recorded with a digital oscilloscope (LeCroy, USA) set at 1 GHz sampling rate and with 1000 averages to improve signal-to-noise ratio for the signal post-processing.

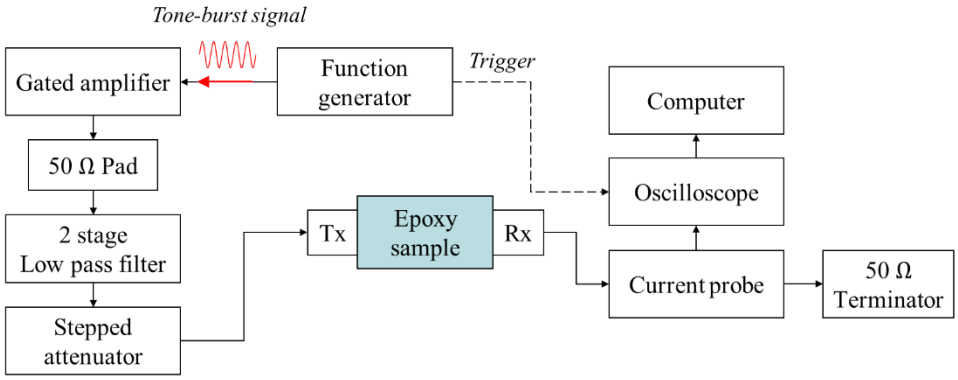

Fig. 4 Trough-transmission experimental setup used for nonlinear measurements

An example of the received time domain signal is shown as Fig. 5 (a). A Hanning window function was applied to the steady-state 15 cycles of the received time domain signal to prevent spectral leakage, which reduces side-lobe effects [48]. When window functions are applied to signals, there can be power loss, so a scaling factor was used to compensate for the amplitude reduction due to the use of the Hanning window. The amplitudes of the fundamental and second harmonics were then obtained using a Fast Furrier Transform (FFT). An example of the measured amplitudes of the fundamental and second harmonic frequencies for the case of the pure sample in the frequency spectrum are given in Fig. 5 (b). By changing the power output using the stepped attenuator, this measurement process to obtain the fundamental and second harmonic components was repeated at several signal power outputs to determine the relationship between the amplitudes of the fundamental and second harmonic frequencies, which enables the nonlinearity parameter (β') to be obtained.

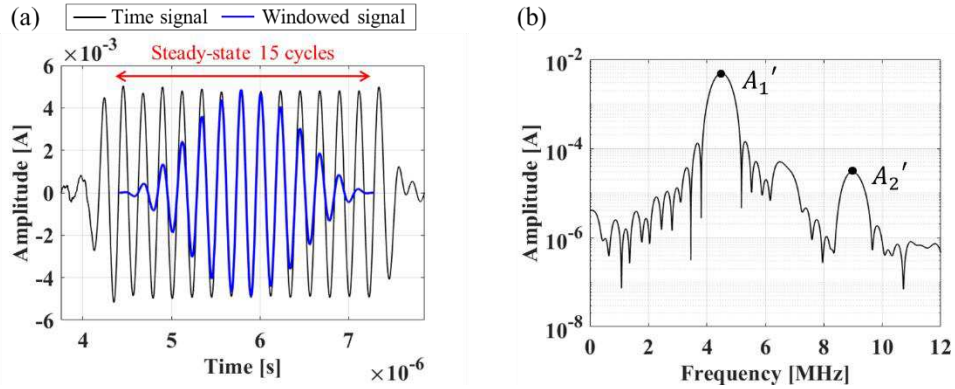

Fig. 5 Example of (**a**) The received time domain signal with Hanning window function, and (**b**) frequency spectrum showing the fundamental and second harmonic components

Fig. 6 (a) shows the nonlinearity parameter (β') as a function of the fundamental amplitude ($A_1{}'$), obtained by changing the power output using the stepped attenuator. For the data shown

in Fig. 6 (a), at small amplitudes the β' value varies, because the second harmonic components are at or below the noise levels. The most reliable descriptor of properties is for the range of the fundamental amplitude which gives the stable region [45] and a consistent nonlinearity parameter. Using the stable region of the fundamental amplitude, a reproducible linear relationship between the square of the fundamental amplitude and second-harmonic amplitude was obtained as shown in Fig. 6 (b). The slope of this relationship gives a value for the nonlinearity parameter that is consistent with the relationship given as equation 5 (b).

This measurement process was repeated three times at each three points on each sample; giving a total of nine measurements for each sample. These data minimize the effect of any micro-bubbles randomly distributed in the samples and the effect of the surface contact conditions between the transducers and samples, and provide more accurate and reliable results.

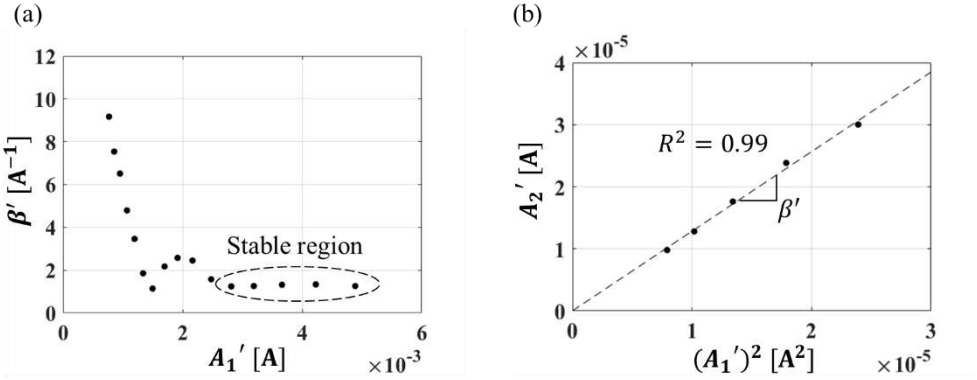

Fig 6 Nonlinearity metrics: (**a**) the relative nonlinearity parameter as a function of the fundamental amplitude, and (**b**) the relationship between the square of the fundamental amplitude and the second harmonic amplitude

4.2 Sound velocity

Sound velocity in the samples was measured using a common pulse-echo method. To generate ultrasonic waves, the pulser/receiver (Olympus 5800, USA) was used, in combination with the 5 MHz and 10 MHz commercial transducers that were employed in the SHG method measurements. For each transducer, the received time domain signal reflected from the opposite side (back-wall) of samples was recorded and an example of a typical signal is shown in Fig. 7. The transit times for the first and second time-of-flight (ToF) signals were measured based on the differences between the first zero-crossing points. The difference between the first and second ToF transit times were then averaged. The measurement was repeated three times at each of three points on each sample. In addition, the data obtained from each 5 MHz and 10 MHz ultrasonic signal was also averaged to get a best estimate of the ToF transit time. The ToF transit time (t) and sample-thickness (d) data were then used to give the sound velocity (c) using equation 6.

$$c = \frac{2 \times d}{t} \ (m/s) \tag{6}$$

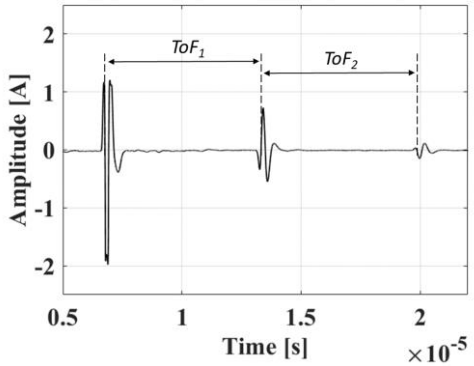

Fig. 7 Example of the pulse-echo signal for 5 MHz transducer: received time domain back-wall echo's showing 1st, 2nd, and 3rd reflections.

4.3 Mechanical hardness

To measure the mechanical hardness of softer non-metallic materials, such as epoxies, Rockwell hardness testing based on M type (HRM) is commonly used [49]. In this study, a Rockwell hardness tester (LECO LR-series, USA) which uses the setup for the M type ball type indenter, with a 100 kg load and a 6.35 mm (¼ inch) ball, was employed. For each sample, the measurement was repeated 10 times on the surface of the sample and averaged.

4.4 Curing reaction and thermal stability

Thermal characteristics of the epoxy samples were analyzed using differential scanning calorimetry (DSC) and thermogravimetric analysis (TGA) performed with a Netzsch STA449 F1 instrument (Netzsch, USA). In DSC, the curing reaction, which is one of critical curing kinetics phenomena, was measured for the epoxy samples cured in alumina crucibles. The measurements gave the glass transition temperature (T_g) in the heating temperature range from room temperature to 400 °C. The temperature, T_g, can give the glass transition point which is used to determine the curing kinetics of epoxies. This temperature was measured at the peak point of the first derivative of DSC results, which has a similar value to the midpoint of the glass transition. In addition, in TGA, the thermal stability was analyzed by measuring two parameters, the initial decomposition temperature (IDT) and the temperature of the maximum rate of degradation (T_{max}), based on the amount of the weight loss in the cured epoxy as a function of a temperature. In the measurements, the IDT was measured at the onset of weight decomposition and the T_{max} was measured at the 50% point for weight loss. The TGA measurements were performed in the heating temperature range from the room temperature to 600 °C. For both DSC and TGA, the heating rate is 10 °C/min under a nitrogen atmosphere of 20 mL/min.

5. Results and discussion

The linear ultrasonic data (sound velocity), and the second harmonic generation data (relative nonlinearity parameter, β') were compared the corresponding results for different samples, specifically the material characterizations that gave mechanical hardness and various thermo-physical properties. In more details, mechanical hardness, and curing reaction and thermal stability were evaluated through the mechanical (hardness) and thermal (glass transition temperature, the initial decomposition temperature, and the temperature of the maximum rate of degradation) parameters for the various samples. Potential correlations between the nonlinearity parameter and material properties of epoxy samples with varying levels of contamination were investigated.

5.1 Effects of contaminant on thermal properties of epoxy-adhesive

The DSC analysis was conducted to investigate the curing behavior of the epoxy-adhesive with varying levels of contamination. Fig. 8 shows the DSC result of four contaminant cases. From these results, the T_g for each contaminant case was calculated and these data are summarized in Table 1. The T_g values of the contaminated materials are lower than that for the pure material, and the T_g value is gradually decreased with the increase in the level of the contaminant. This trend means that the contaminant would appear to slow the curing reaction of the epoxy mixture, because the partial weight of the contaminant can be miscible with the epoxy during the curing process. If the curing reaction decreases due to the contaminant and there is unreacted epoxy in the mixture in the cured state, the cross-linking density would also be decreased, which reduces the chemical rigidity of the epoxy network. It appears that it can be assumed that the contaminant can retard the rate of the curing reaction and deteriorate the physical/chemical properties of the epoxy system.

The TGA analysis was conducted to investigate the effect of the contaminant on the thermal stability of the epoxy-adhesive. The TGA results, the weight loss as a function of the temperature, are shown in Fig. 9. To determine the thermal stability of the material, also known as the thermal degradation behavior, the IDT and the T_{max} were used as indicators. The values of these two temperatures with varying levels of contamination are summarized in Table 1. From the data it is seen that the IDT of the contaminated materials are definitely lower than that of the pure material. The contaminated cases have a similar value of IDT, which is not unreasonable given that the differences between the contamination levels is small, and this results in only very small changes in the initial decomposition range. These results do show that the pure epoxy has a better epoxy network. Also, the T_{max} is gradually decreased with the increased in the level of the contaminant. After the initial decomposition range, the higher the level of contamination the higher the thermal decomposed. Based on the decrease in the IDT and T_{max} with the increased in the level of contamination, the TGA results can also confirm that it is highly likely that the contaminant can induce the incomplete curing reaction of the epoxy mixture, and therefore decrease the cross-linking density. Both DSC and TGA results show that the contaminant can deteriorate the thermal properties of the epoxy-adhesive.

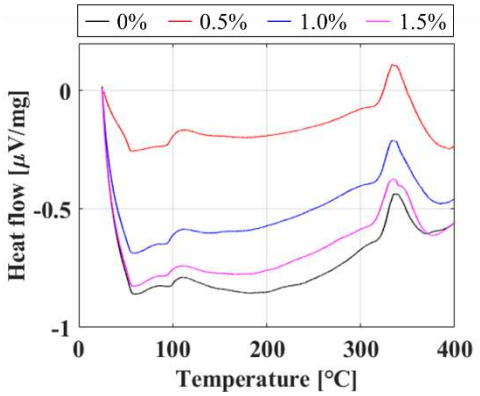

Fig. 8 DSC results of four contamination levels

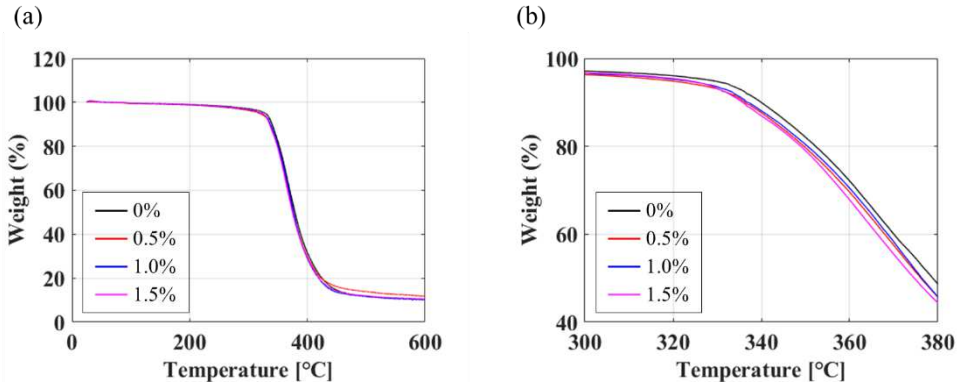

Fig. 9 TGA results (**a**) four contamination levels, and (**b**) data shown on expanded scales between 300℃ and 380℃

Table 1 Curing reaction and thermal stabilities of samples as a function of the contamination level

Contamination level	DSC	TGA	
	T_g (℃)	IDT (℃)	T_{max} (℃)
0%	99.86	339.6	378.1
0.5%	97.04	335.4	376.4
1.0%	96.17	336.7	376.2
1.5%	95.60	336.1	375.1
ΔT Error	± 1℃		

5.2 Effects of the contaminant on ultrasonic parameters

The sound velocity (c) and the relative nonlinearity parameter (β') were measured and data compared for the epoxy-adhesive samples with varying level of contamination. The effects of the contaminant on ultrasonic characteristics are shown in Fig. 10. In the comparison, the sound

velocity is seen to decrease, and the normalized nonlinearity parameter (β'/β_0') increases with the increase in the level of contamination. With the decreased trend of the sound velocity, if the mechanical hardness is decreased with the increased level of the contamination, it can be assumed that the contaminant can induce material softening in the epoxy-adhesive. Modulus of elasticity (E) is proportional to the sound velocity, and the modulus and the mechanical hardness (H) are related to each other.

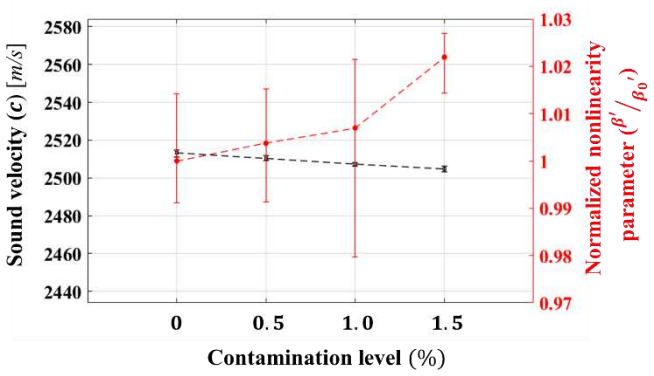

Fig. 10 Comparison between changes in the sound velocity (c) and the normalized nonlinearity parameter (β'/β_0') with varying the levels of contamination

To confirm this relationship, the effect of the contaminant on mechanical hardness of the epoxy-adhesive was investigated. With the increased level of the contaminant, the hardness of the epoxy-adhesive is decreased as shown in Fig. 11. This result confirms that the contaminant can induce material softening of the epoxy-adhesive, which in turn decreases the sound velocity.

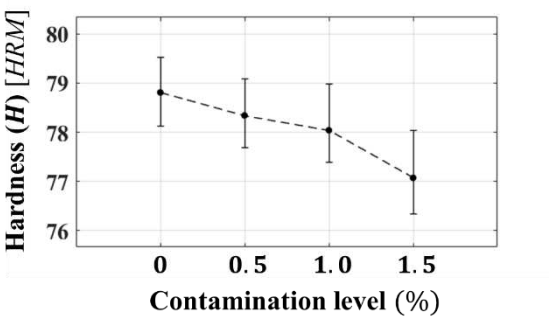

Fig. 11 Mechanical hardness (H) with varying level of contamination

In reviewing the data, the nonlinearity parameter, shown in Fig. 10, is seen to increase with increased contamination. This change correlates with the expected micro-structural change in

the epoxy-adhesive due to the contaminant. When the contaminant causes the slower curing reaction in the epoxy-adhesive, there will be incomplete curing and impurities generated in the cured epoxy-adhesive. These impurities can be related to the micro-structural change in the epoxy-adhesive, which means the increased impurities due to the contaminant will cause the increase of the nonlinearity parameter.

In addition, the sensitivity to changes in the contamination level was compared for the sound velocity and the normalized nonlinearity parameter. While the rate of change in the sound velocity is only 0.33% from the pure case to the 1.5% contamination level, the normalized nonlinearity parameter is changed by 2.15% as shown in Fig. 10.

It can be seen that the nonlinearity parameter has the potential, in at least this case, to detect the level of contamination. The effect on β' is seen to be 6.5 times larger than the corresponding change seen in the sound velocity. The sensitivity comparison of ultrasonic parameters was also extended to consider –the mechanical hardness. The rate of change of the hardness from the pure case to the 1.5% contamination level is about 2.16% as shown in Fig. 11. This trend is in good agreement with that seen for the nonlinearity parameter, which shows a good correlation between the changes in the nonlinearity parameter and the hardness.

5.3 Correlations between nonlinearity parameter and the mechanical, and thermal properties

The effects of contaminant showed that the perturbation of the chemical reactions, by the contamination, in the epoxy system were seen in the changes in the mechanical degradation of the epoxy-adhesive. To investigate the relationships between the nonlinearity parameter and the degradation of material properties for the epoxy-adhesive due to the contaminant, possible correlations were investigated.

The parameters related to the thermal and mechanical properties of the epoxy-adhesive and the nonlinearity parameter were normalized to enable more convenient comparison and these normalized values are shown in Fig. 12. The changes in nonlinearity parameter show a good correlation with the thermal and mechanical properties with varying level of contaminant. If the thermal and mechanical properties of the epoxy-adhesive are gradually degraded by the contaminant, the nonlinearity parameter is seen to have a proportionally increase due to the degree of degradation. On the basis of this correlation, it can be assumed that the SHG method using the relative nonlinearity parameter (β') can potentially be used to nondestructively measure the effect of the contaminant on the thermal and mechanical properties of the epoxy-adhesive.

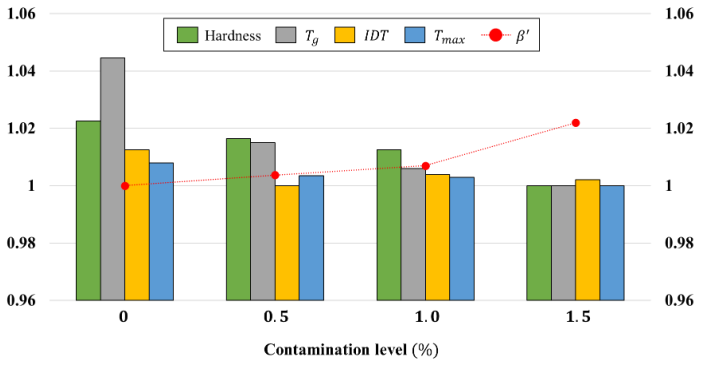

Fig. 12 Relationships between the nonlinearity parameter and material properties of the epoxy-adhesive with different levels of contamination.

6. Conclusions

This study demonstrates that the SHG method using the nonlinearity parameter (β') can potentially be used to evaluate the effect of a contaminant on the material properties of an epoxy-adhesive. The experimental results show that the nonlinearity parameter has higher sensitivity to the level of contamination than the sound velocity. In addition, the changes in the nonlinearity parameter, with varying level of the contamination, are seen to correlate well with changes in the mechanical hardness. Thermal analyses also showed that the increased level of the contaminant gradually degrades the curing reaction and the thermal stability of the epoxy-adhesive, which correlates with increases in the nonlinearity parameter. The observed correlation between the nonlinearity parameter and mechanical, and thermal characteristics of the epoxy adhesive with varying degrees of contaminant demonstrates that the nonlinearity parameter has potential as a quantitative nondestructive method for use to evaluate the bond quality of the epoxy-adhesive.

Acknowledgement

This research is supported, in part, by a R. Bruce Thompson Graduate Fellowship in Center for Nondestructive Evaluation (CNDE) in Iowa State University. The authors include as a co-author Lucas Koester who contributed to this work. He died unexpectedly (March 16, 2022) just before this paper was completed. Lucas was a great field and colleague who will be greatly missed by all who knew him.

References

[1] Sulejmani, S., Sonnenfeld, C., Geernaert, T., Luyckx, G., Mergo, P., Urbanczyk, W., Karima, C., Thienpont, H., Berghmans, F.: Disbond monitoring in adhesive joints using shear stress optical fiber sensors. Smart materials and structures. **23**(7), 075006 (2014)

[2] Banea, M. D., Rosioara, M., Carbas, R. J. C., Da Silva, L. F. M.: Multi-material adhesive joints for automotive industry. Composites Part B: Engineering. **151**, 71-77 (2018)

[3] Guyott, C. C. H., Cawley, P., Adams, R. D.: The non-destructive testing of adhesively bonded structure: a review. The Journal of Adhesion. **20**(2), 129-159 (1986)

[4] Jhang, K. Y., Lissenden, C. J., Solodov, I., Ohara, Y., Gusev, V. (Eds.).: Measurement of nonlinear ultrasonic characteristics. Springer, Singapore (2020)

[5] Yan, D., Drinkwater, B. W., Neild, S. A.: Measurement of the ultrasonic nonlinearity of kissing bonds in adhesive joints. NDT & E International. **42**(5), 459-466 (2009)

[6] Nagy, P. B.: Ultrasonic detection of kissing bonds at adhesive interfaces. Journal of Adhesion Science and Technology. **5**(8), 619-630 (1991)

[7] Kundu, T., Maji, A., Ghosh, T., Maslov, K.: Detection of kissing bonds by Lamb waves. Ultrasonics. **35**(8), 573-580 (1998)

[8] Alston, J., Croxford, A., Potter, J., Blanloeuil, P.: Nonlinear non-collinear ultrasonic detection and characterization of kissing bonds. NDT & E International. **99**, 105-116 (2018)

[9] Brotherhood, C. J., Drinkwater, B. W., Guild, F. J.: The effect of compressive loading on the ultrasonic detectability of kissing bonds in adhesive joints. Journal of Nondestructive Evaluation. **21**(3), 95-104 (2002)

[10] Roach, D., Rackow, K., Duvall, R.: Innovative use of adhesive interface characteristics to nondestructively quantify the strength of bonded joints. In Proceedings of the 10th European Conference on Non-destructive Testing. Moscow 3263-3277 (2010)

[11] Biwa, S., Hiraiwa, S., Matsumoto, E.: Experimental and theoretical study of harmonic generation at contacting interface. Ultrasonics. **44**, e1319-e1322 (2006)

[12] Nagy, P. B.: Ultrasonic detection of kissing bonds at adhesive interfaces. Journal of Adhesion Science and Technology. **5**(8), 619-630 (1991)

[13] Jeenjitkaew, C., Guild, F. J.: The analysis of kissing bonds in adhesive joints. International Journal of Adhesion and Adhesives. **75**, 101-107 (2017)

[14] Marty, P. N., Desai, N., Andersson, J.: NDT of kissing bond in aeronautical structures. In Proceedings of the 16th World Conference on NDT. (2004).

[15] Jeenjitkaew, C., Luklinska, Z., Guild, F.: Morphology and surface chemistry of kissing bonds in adhesive joints produced by surface contamination. International Journal of Adhesion and Adhesives. **30**(7), 643-653 (2010)

[16] Maeva, E., Severina, I., Bondarenko, S., Chapman, G., O'Neill, B., Severin, F., Maev, R. G.: Acoustical methods for the investigation of adhesively bonded structures: A review. Canadian Journal of Physics, **82**(12), 981-1025 (2004)

[17] Ehrhart, B., Ecault, R., Touchard, F., Boustie, M., Berthe, L., Bockenheimer, C., Valeske, B.: Development of a laser shock adhesion test for the assessment of weak adhesive bonded CFRP structures. International Journal of Adhesion and Adhesives. **52**, 57-65 (2014)

[18] Wood, M., Charlton, P., Yan, D.: Ultrasonic evaluation of artificial kissing bonds in CFRP composites. The e-Journal of NDT. **19**(12) (2014)

[19] Tighe, R. C., Dulieu-Barton, J. M., Quinn, S.: Identification of kissing defects in adhesive bonds using infrared thermography. International Journal of Adhesion and Adhesives. **64**, 168-

178 (2016)

[20] Kumar, R. V., Bhat, M. R., Murthy, C. R. L.: Evaluation of kissing bond in composite adhesive lap joints using digital image correlation: Preliminary studies. International Journal of Adhesion and Adhesives. **42**, 60-68 (2013)

[21] Wang, P., Li, Z., Zhou, L., Pei, Y.: Microwave nondestructive detection and quantitative evaluation of kissing defects in GFRP laminates. Composites Science and Technology, **162**, 117-122 (2018)

[22] Chen, B. Y., Soh, S. K., Lee, H. P., Tay, T. E., Tan, V. B.: A vibro-acoustic modulation method for the detection of delamination and kissing bond in composites. Journal of Composite Materials. **50**(22), 3089-3104 (2016)

[23] Jhang, K. Y.: Nonlinear ultrasonic techniques for nondestructive assessment of micro damage in material: a review. International Journal of Precision Engineering and Manufacturing. **10**(1), 123-135 (2009)

[24] Solodov, I. Y., Krohn, N., Busse, G.: CAN: an example of nonclassical acoustic nonlinearity in solids. Ultrasonics. **40**(1-8), 621-625 (2002)

[25] Van Den Abeele, K. A., Johnson, P. A., Sutin, A.: Nonlinear elastic wave spectroscopy (NEWS) techniques to discern material damage, part I: nonlinear wave modulation spectroscopy (NWMS). Journal of Research in Nondestructive Evaluation. **12**(1), 17-30 (2000)

[26] Van Den Abeele, K. E., Sutin, A., Carmeliet, J., Johnson, P. A.: Micro-damage diagnostics using nonlinear elastic wave spectroscopy (NEWS). NDT & E International. **34**(4), 239-248 (2001)

[27] Ohara, Y., Mihara, T., Yamanaka, K.: Effect of adhesion force between crack planes on subharmonic and DC responses in nonlinear ultrasound. Ultrasonics. **44**(2), 194-199 (2006)

[28] Richardson, J. M.: Harmonic generation at an unbonded interface—I. Planar interface between semi-infinite elastic media. International Journal of Engineering Science. **17**(1), 73-85 (1979)

[29] Zhang, Z., Nagy, P. B., Hassan, W.: Analytical and numerical modeling of non-collinear shear wave mixing at an imperfect interface. Ultrasonics. **65**, 165-176 (2016)

[30] Kim, J., Jhang, K. Y., Kim, C.: Dependence of nonlinear ultrasonic characteristic on second-phase precipitation in heat-treated Al 6061-T6 alloy. Ultrasonics. **82**, 84-90 (2018)

[31] Metya, A., Ghosh, M., Parida, N., Sagar, S. P.: Higher harmonic analysis of ultrasonic signal for ageing behaviour study of C-250 grade maraging steel. NDT & E International. **41**(6), 484-489 (2008)

[32] Cantrell, J. H.: Substructural organization, dislocation plasticity and harmonic generation in cyclically stressed wavy slip metals. Proceedings of the Royal Society of London. Series A: Mathematical, Physical and Engineering Sciences. **460**(2043), 757-780 (2004)

[33] Nagy, P. B.: Fatigue damage assessment by nonlinear ultrasonic materials characterization.

570 Ultrasonics. **36**(1-5), 375-381 (1998)

571 [34] Shui, G., Wang, Y. S., Huang, P., Qu, J.: Nonlinear ultrasonic evaluation of the fatigue
572 damage of adhesive joints. NDT & E International. **70**, 9-15 (2015)

573 [35] Cantrell, J. H., Yost, W. T.: Nonlinear ultrasonic characterization of fatigue microstructures.
574 International Journal of Fatigue. **23**, 487-490 (2001)

575 [36] Ruiz, A., Ortiz, N., Medina, A., Kim, J. Y., Jacobs, L. J.: Application of ultrasonic methods
576 for early detection of thermal damage in 2205 duplex stainless steel. NDT & E International.
577 **54**, 19-26 (2013)

578 [37] Balasubramaniam, K., Valluri, J. S., Prakash, R. V.: Creep damage characterization using
579 a low amplitude nonlinear ultrasonic technique. Materials Characterization, **62**(3), 275-286
580 (2011)

581 [38] Barnard, D. J., Dace, G. E., Rehbein, D. K., Buck, O.: Acoustic harmonic generation at
582 diffusion bonds. Journal of Nondestructive Evaluation. **16**(2), 77-89 (1997)

583 [39] Brotherhood, C. J., Drinkwater, B. W., Dixon, S.: The detectability of kissing bonds in
584 adhesive joints using ultrasonic techniques. Ultrasonics. **41**(7), 521-529 (2003)

585 [40] Pyun, D-K, Koester, L.W., Barnard, D.J. and Bond, L.J. (2022) Nonlinear ultrasonic
586 inspection of cohesive failure in adhesive due to contaminants in the manufacturing process ;
587 Proceedings SPIE Conference 12047, Nondestructive Characterization and Monitoring of
588 Advanced Materials, Aerospace, Civil Infrastructure, and Transportation XVI, 7 - 9 March
589 2022 Paper # 12047-10 |(In Press)
590

591 [41] Park, S. J., Jin, F. L., Lee, J. R.: Thermal and mechanical properties of tetrafunctional
592 epoxy resin toughened with epoxidized soybean oil. Materials Science and Engineering: A.
593 **374**(1-2), 109-114 (2004)

594 [42] Yin, H., Jin, H., Wang, C., Sun, Y., Yuan, Z., Xie, H., Xie, H., Wang, Z., Cheng, R.:
595 Thermal, damping, and mechanical properties of thermosetting epoxy-modified asphalts.
596 Journal of Thermal Analysis and Calorimetry. **115**(2), 1073-1080 (2014)

597 [43] Jhang, K. Y.: Applications of nonlinear ultrasonics to the NDE of material degradation.
598 IEEE transactions on ultrasonics, ferroelectrics, and frequency control. **47**(3), 540-548 (2000)

599 [44] Dace, G. E., Thompson, R. B., Buck, O.: Measurement of the acoustic harmonic
600 generation for materials characterization using contact transducers. Review of Progress in
601 Quantitative Nondestructive Evaluation, Vol. 11B, 2069-2076 (1992)

602 [45] Chakrapani, S. K., Howard, A., Barnard, D.: Influence of surface roughness on the
603 measurement of acoustic nonlinearity parameter of solids using contact piezoelectric
604 transducers. Ultrasonics. **84**, 112-118 (2018)

605 [46] Shui, G., Song, X., Xi, J., Wang, Y. S.: Experimental characterization of impact fatigue
606 damage in an adhesive bonding using the second harmonics. Journal of Nondestructive
607 Evaluation. **36**(2), 23 (2017)

608 [47] Cole, K. C.: A new approach to modeling the cure kinetics of epoxy/amine thermosetting
609 resins. 1. Mathematical development. Macromolecules. **24**(11), 3093-3097 (1991)

610 [48] Blanloeuil, P., Meziane, A., Bacon, C.: Numerical study of nonlinear interaction between
611 a crack and elastic waves under an oblique incidence. Wave Motion. **51**(3), 425-437 (2014)

612 [49] Gopinath, A., Kumar, M. S., Elayaperumal, A.: Experimental investigations on mechanical
613 properties of jute fiber reinforced composites with polyester and epoxy resin matrices. Procedia
614 Engineering. **97**, 2052-2063 (2014)